

MODEL FOR HIGH TEMPERATURE PHASE OF C₇₀ SOLID

Sarbpreet Singh, K. Dharamvir and V.K. Jindal¹
Department of Physics, Panjab University, Chandigarh-160014, India

ABSTRACT

Depending on the temperature, the C₇₀ solid crystallizes in several structures. At high temperature ($T > 340\text{K}$), the ellipsoidal C₇₀ molecule rotates freely in all directions and may be treated as a uniform thick spherical shell with inner and outer radii as the minimum and the maximum distance of C-atom from the center of the molecule. At lower temperatures the free rotations of molecules freeze out. We have calculated the lattice parameters, energies and bulk modulus at the minimum energy configuration of fcc and hcp phase of pure C₇₀ solid at high temperature using a simple model based on atom-atom potential.

INTRODUCTION

Carbon is a remarkable element showing a variety of stable forms. Fullerenes are often referred as third form of carbon, others being diamond and graphite. The word “fullerene” is used to denote the whole class of closed cage molecules consisting of only carbon atoms. The most abundantly known fullerene consists of 60 carbon atoms and the solid popularly known as C₆₀ solid. The C₆₀ solid has been extensively studied both theoretically and experimentally. Another fullerene solid consisting of molecules comprising of 70 atoms of carbon, known as C₇₀ solid is also found in good abundance. As the molecular weight increases beyond C₇₀, the abundance decreases dramatically.

Whereas C₆₀ molecule is nearly spherical in shape with all the carbon atoms located at the vertices of a truncated icosahedron having 60 vertices, the molecule of C₇₀ is more like a rugby ball. The C₇₀ molecule can be envisioned by adding a ring of 10 carbon atoms or,

¹ Author with whom correspondence be made, jindal@panjabuniv.chd.nic.in

equivalently, adding a belt of five hexagons around the equatorial plane of C_{60} molecule which is normal to one of the five fold axes and rotating the two hemisphere of C_{60} so that they fit continuously onto the belt hexagons [1] as shown in fig.1.

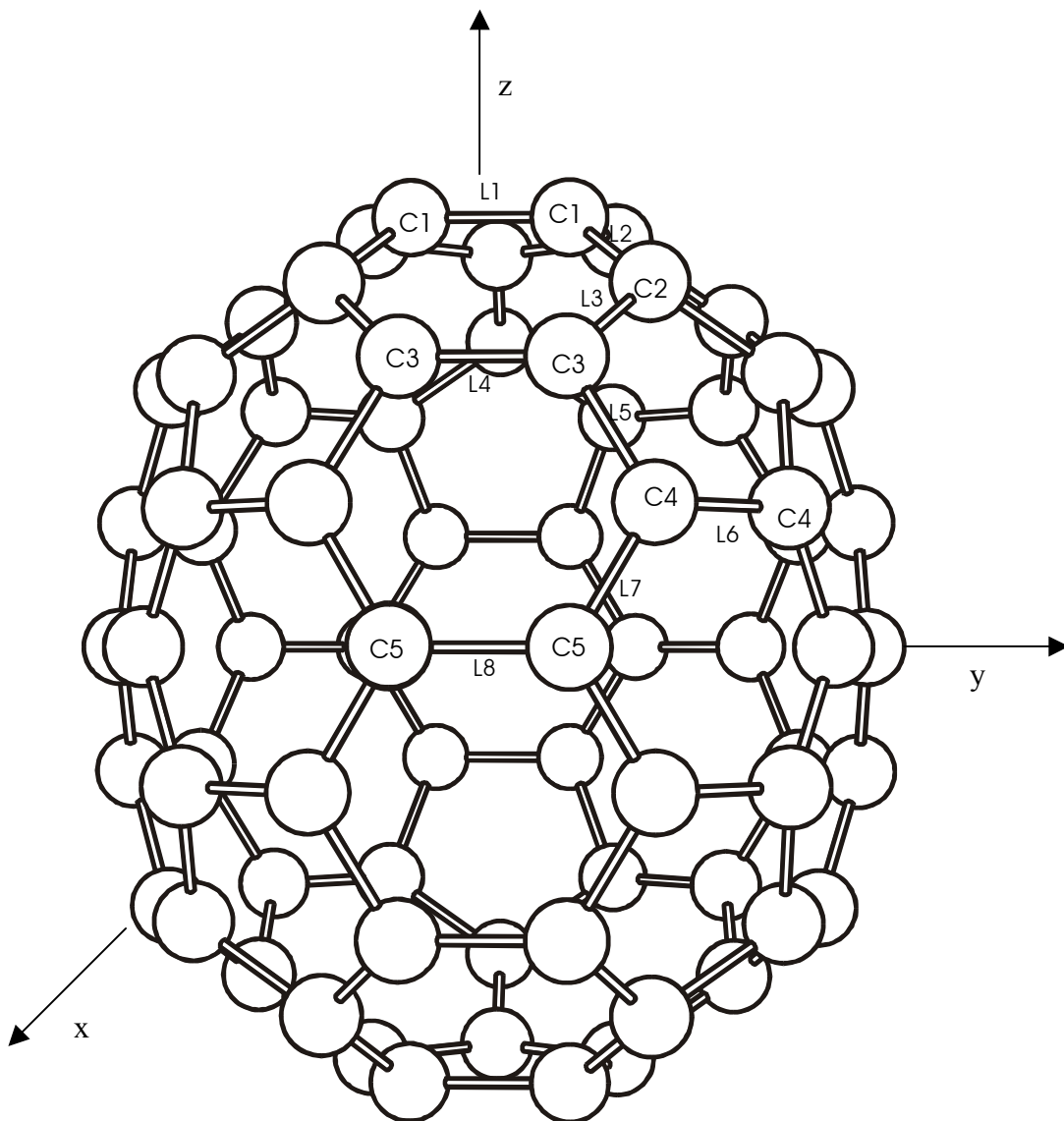


Fig.1 The C_{70} molecule with circles representing the C-atoms

For C_{60} the stacking sequence is ABCABC..., at all temperatures, thus the crystal structure are face-centered cubic (fcc) and simple cubic (sc). Above room temperature, the C_{60} molecules are spinning rapidly about their lattice positions and there is no orientational

order and the solid crystallizes into a fcc phase. As the temperature is lowered below room temperature, the free rotations freeze and the system undergoes a phase transition from fcc to sc. For C_{70} , both ABCABC.... and ABAB.... sequences are observed and hence the crystal structures are fcc or hcp depending on the temperature range.

Several experimental observations have been made to study the structure[2,3] and phase transitions[1] in C_{70} . Bulk and the thermodynamical properties of C_{70} solid have also been experimentally measured[4]. Theoretical models for fullerene solids are generally based on model potentials for C-C interaction which are then summed over to obtain molecule-molecule potentials. Generally, the fullerene molecules are considered to be stiff and rigid while in the solid. Although some calculations[5] have been done based on molecular-dynamics calculations(MD) to study the structural properties of C_{70} using Lennard-Jones potential, an exercise needs to be attempted for the detailed temperature and pressure effects and to assess the usefulness of the simple model chosen here. A simple model based approach would be very useful for calculations of various bulk, lattice and thermodynamic properties and thus provides a quick comparison with the measured results.

PHASE TRANSITIONS IN C_{70}

Depending on the temperature, C_{70} solid has been found to crystallize in various crystal phases[6]. At high temperatures ($T > 340\text{K}$), solid C_{70} shows no long-range orientational order of its molecules. In this temperature regime, the fcc phase with freely rotating molecules is the most stable phase with ideal hexagonal closed packed phase almost equally stable. The molecular centers are arranged on fcc lattice with four C_{70} molecules per unit cell and on hcp lattice with two molecules per unit cell. As the temperature is lowered below $T_{01}(=340\text{K})$, a phase transition to a phase with long-range orientational order of the molecules takes place. In this temperature range, the C_{70} molecules rotate only about the five fold axis. In this range, the long-range orientational order breaks the cubic symmetry and the crystal distorts into a rhombohedral lattice. As the temperature is further lowered below $T_{02}(=280\text{K})$, the free rotation about the long axis also becomes frozen and the crystal phase below this temperature is a monoclinic structure. In the intermediate temperatures the C_{70} molecule may, therefore, be modeled as an ellipsoid of revolution which on further increase

in temperature above T_{01} can be modeled as a spherical shell. Various possible structures for C_{70} at different temperature ranges have been summarized in fig.2.

Fig.2 Various structures of C_{70} in different temperature ranges[6].

Low temperature phase ($T < 280$ K)	Intermediate temperature phase ($280 \text{ K} < T < 340$ K)	High temperature phase ($T > 340$ K)
Monoclinic Molecular orientations ordered	Rhombohedral Molecules rotate about long axis.	fcc and hcp Disordered molecular orientations

THEORETICAL MODEL AND CALCULATIONS

General Interaction Model

The knowledge of the interaction potential is the basic ingredient to calculate the bulk, structural and dynamical properties of any system. Following our earlier success in modeling C-cluster molecular solids, we assume that atom-atom potential govern the inter-molecular potential in C_{70} solids also. The intermolecular potential energy $U_{l\kappa, l'\kappa'}$ between the two C_{70} molecules identified by κ molecule in unit cell l , κ' molecule in cell l' , can be written[7] as

$$U_{l\kappa, l'\kappa'} = \sum_{ij} V(r_{ij}) \quad (1)$$

where r_{ij} is the distance between C-atom of molecules $l\kappa$ and $l'\kappa'$. In case of C_{70} the summation includes all the 70 atoms in each of the molecules and $V(r)$ is the C-C potential for the two C atoms situated at r distance apart, and is of the form

$$V(r) = -\frac{A}{r^6} + B \cdot \exp(-\alpha r) \quad (2)$$

The interaction parameters A , B and α are taken from the set provided by Kitaigorodski, which have already been used successfully[7].

From the knowledge of the crystal structure which provides the lattice positions, the total potential energy Φ can be obtained numerically by carrying out the lattice sums. In order to obtain the total potential energy Φ , we need to sum $U_{l\kappa, l'\kappa'}$ (Eq. (1)) for all pair-wise

molecular interactions. For this summation, we need all the atom-atom distances between various molecules.

$$\Phi = \frac{1}{2} \sum_{l\kappa, l'\kappa'} U_{l\kappa, l'\kappa'} \quad (3)$$

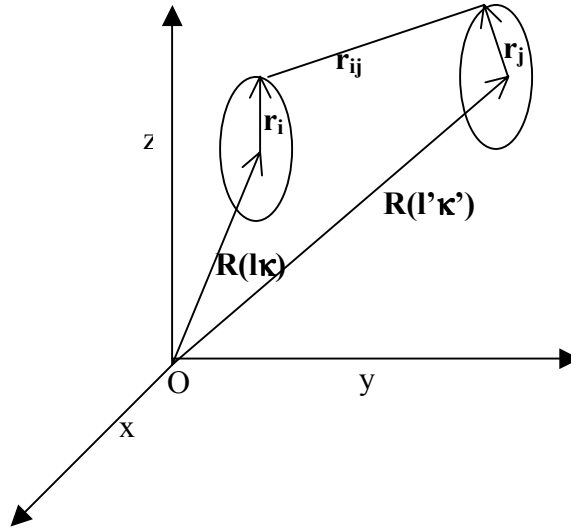


Fig.3 Diagram representing the positions of i^{th} and j^{th} atoms on two different C_{70} molecules.

Knowing the position vectors of the centers of the molecules as $\mathbf{R}(l\kappa)$ and $\mathbf{R}(l'\kappa')$, and atomic vectors \mathbf{r}_i and \mathbf{r}_j , the atom-atom distance $r_{ij}(l\kappa, l'\kappa')$, as shown in fig.3, is written as

$$r_{ij}(l\kappa, l'\kappa') = | \mathbf{R}(l'\kappa') + \mathbf{r}_j - \mathbf{R}(l\kappa) - \mathbf{r}_i | \quad (4)$$

Therefore, knowing the crystal structure ($\mathbf{R}(l\kappa)$) and knowing the atomic coordinates of C_{70} from the molecular geometry, the atom-atom distances can be obtained which finally leads to the total potential energy (Eq. (3)).

In C_{70} molecule there are five inequivalent carbon sites (C_1, C_2, \dots, C_5) and eight distinct bond lengths (L_1, L_2, \dots, L_8) as shown in fig.1. These eight bond lengths found experimentally by neutron inelastic scattering (NIS) [8] are listed Table 1.

Table 1 Experimental bond lengths of C_{70} (in Å)

Bond	C ₁ -C ₁	C ₁ -C ₂	C ₂ -C ₃	C ₃ -C ₃	C ₃ -C ₄	C ₄ -C ₄	C ₄ -C ₅	C ₅ -C ₅
NIS	1.460	1.382	1.449	1.396	1.464	1.420	1.415	1.477

Various groups have also calculated these lengths using tight binding molecular dynamics (TBMO)[9], the local density approximation (LDA)[10], modified neglect of differential overlap(MNDO)[11] and Hartree-Fock(HA) methods and got the bond lengths ranging from 1.356Å to 1.475Å.

We have generated the atomic coordinates of C_{70} by adding a belt of five hexagons around the equatorial plane of C_{60} molecule which is normal to one of the five fold axes and rotating the two hemisphere of C_{60} so that they fit continuously onto the belt hexagons and considering only two types of bond lengths with single and double bond lengths as 1.40Å and 1.45Å. From the coordinates so obtained it has been observed that the distance of the nearest and the farthest carbon atoms from the center of the C_{70} molecule taken as the semi minor and the semi major axis are $a = 3.498\text{Å}$ and $b = 4.112\text{Å}$ respectively.

Free rotation model

For the case of freely rotating molecules at high temperatures above 340K, as in our case, the orientational correlation vanishes and the molecules rotate freely in all directions. We model the C_{70} molecule by assuming all the 70 C-atoms to be distributed uniformly within a thick spherical shell of inner and outer radii as the semi minor and the semi major axis of the C_{70} molecule, with density ρ as shown in fig.4.

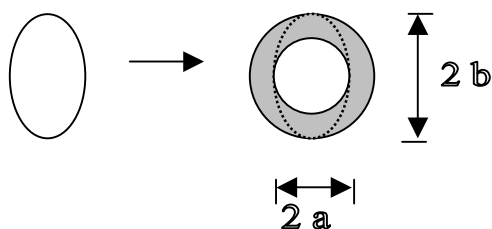


Fig.4 High T equivalent spherical thick shell C_{70} molecule

The density can be calculated as $\rho = 70/\Delta V$, where ΔV is the volume of the thick shell enclosing the 70 carbon atoms and is given by $\Delta V = \frac{4}{3}\pi(b^3 - a^3)$. In this case of free rotation of molecules, the summation over all the 70 atoms in each of the molecules can be replaced by the integration over the spherical shells. The interaction between the two C_{70}

shells can be calculated by considering a small volume element dV_1 on one shell with position vector \mathbf{r}_1 and dV_2 on another shell with position vector \mathbf{r}_2 (Fig.3) and can be written as

$$V(R, a, b) = \iint (\rho dV_1)(\rho dV_2) \left[-\frac{A}{|\mathbf{r}_2 - \mathbf{r}_1|^6} + B \exp(-\alpha |\mathbf{r}_2 - \mathbf{r}_1|) \right] \quad (5)$$

In this way the expression for V has been analytically obtained which is a function of R , the distance of separation of the centers of the two C_{70} thick spherical shells and their geometrical parameters, a and b . The evaluation of the final expression has been described in the appendix.

The summation over various lattice points is obtained for intermolecular distances up to some distance R_L . The potential energy as a function of R_L has been plotted in fig.5 which shows good convergence ($\sim 7 \times 10^{-5} \%$) when the summation is restricted to the distances upto 85 Å. In our calculations the summation up to a intermolecular distances of 90 Å has been done.

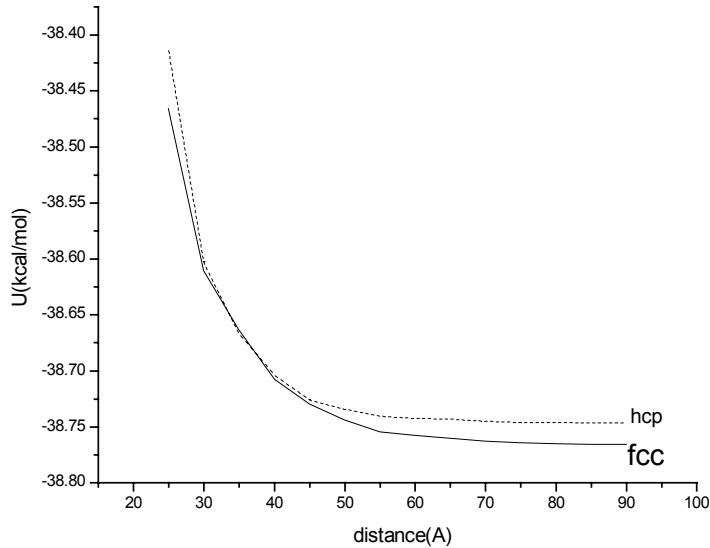


Fig.5 Potential energy as a function of the distance of summation.

The potential energy thus obtained as a function of lattice parameter has been plotted in fig.6. The lattice parameters (a) corresponding to the minimum potential energy and the minimum energy (Φ) for the equilibrium configuration for both the fcc and hcp systems are presented in Table 2. In this table we also present the results from the molecular-dynamics (MD)

calculations done by Pickholz *et. al.*[5] and the experimental results for comparison. Here in our calculations the hcp structure has been taken to be ideal with c/a ratio as 1.63.

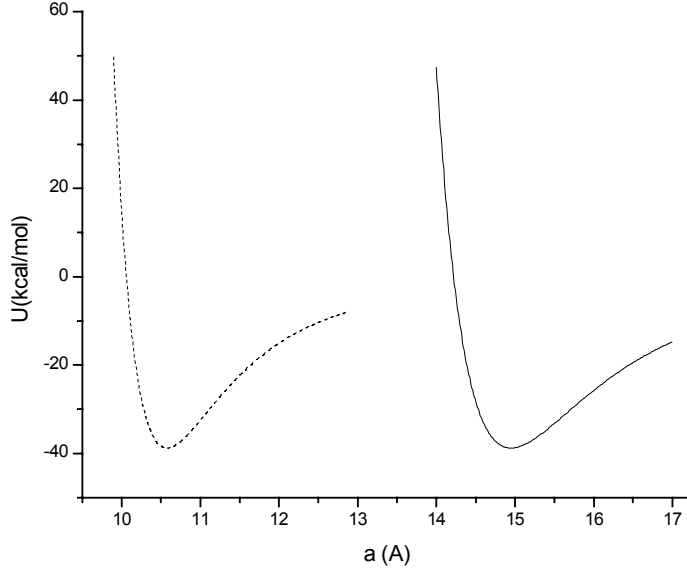


Fig.6 Calculated potential energy of the C_{70} solid as a function of lattice parameter for fcc and hcp structures at high temperatures. The broken line is hcp and continuous line is fcc result.

Table.2 Calculated and experimental structure and energies for C_{70} lattice

Structure	Lattice parameters (Å)			Potential energy (kcal/mol)		
	Our calc.	Exp. ^[2-3]	Other calc. ^[5]	Our calc. (at 739K)	Exp. ^[12] (at 739K)	Other calc. ^[5] (at 739K)
Fcc	a =14.96	15.01	14.80(at room Temp.)	38.76	43.06	44.74
Hcp	a =10.58 c = 17.25	10.56 17.23	10.20(at 200K)	38.74	43.02	44.70

We compare the numerical results for the various physical quantities obtained for pure C_{70} solid at high temperature phase using a simplified model based on atom-atom potentials. Comparison of the calculated lattice parameters (a) and potential energies (Φ) with the experimental values and other calculations done by Pickholz *et. al.* [5], reveals that the present calculation is able to reproduce the structure and cohesive energies quite well for both the fcc and hcp structures. Comparing the calculated potential energies for fcc and hcp structures it is found that fcc phase has energy lower than hcp phase by only 0.05%.

Bulk Modulus

The potential energy varies with the application of the hydrostatic pressure ‘p’ such that

$$\Phi_p = \Phi + p\Delta V \quad (6)$$

where Φ_p is the total potential energy of the system at pressure p and ΔV is the change in the volume of unit cell per molecule of C_{70} because of the application of the pressure. Therefore, bulk modulus $B (= -V\partial p / \partial V)$ can be calculated at minima by knowing the p-V curve for the minimized new potential energy. The plot of volume of unit cell per molecule as a function of pressure for both the systems (fcc and hcp) are presented in Fig.7. The calculated bulk modulus for both fcc and hcp structures are presented in Table 3. The volume of unit cells per molecule for fcc and hcp structures at minimum energy configuration at p=0 are also tabulated in Table 3.

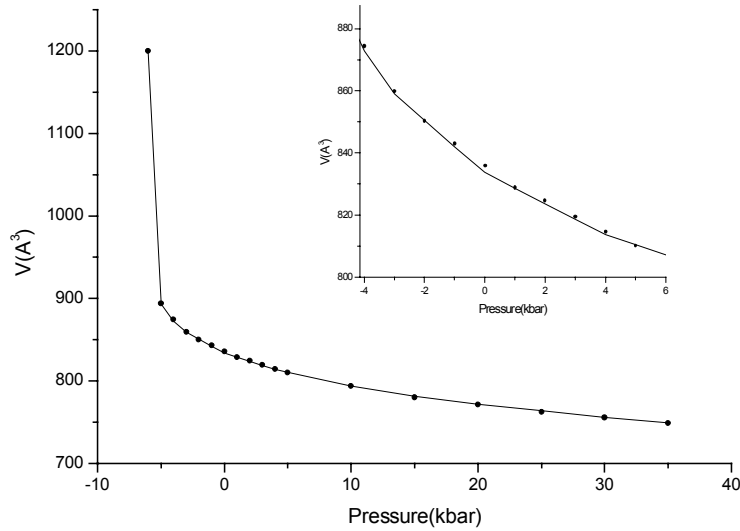


Fig.7 Calculated volume per molecule of the C_{70} as a function of pressure for fcc and hcp structures at high temperatures. The dots represent hcp and continuous line is fcc result.

Table.3 Calculated bulk modulus for C_{70} lattice at high temperatures.

Structure	Bulk Modulus (GPa)		Unit cell volume per molecule (\AA^3)
	p=0	p=30 kbar	
Fcc	13.26	104.9	835.3
Hcp	13.02	103.2	835.9

SUMMARY AND DISCUSSION

We calculated the numerical values for the various physical quantities like lattice parameters (a), potential energies (Φ) and the bulk modulus for pure C_{70} solid at high temperature phase using a simplified model based on atom-atom potentials and compared them with some of the known experimental values and other calculations. For C_{70} solid at high temperatures, fcc phase has energy lower than hcp phase by only 0.05%. Thus we can conclude that fcc structure is slightly more stable than ideal hcp structure. Though no experimental data was available for comparison of the bulk modulus, however the bulk modulus on comparison with C_{60} solid [7] shows that the C_{70} solid is more compressible.

Further in order to calculate the lattice dynamics, internal vibrational modes would need to be included. Also for intermediate and low temperature, the C-atoms can no longer be assumed to be distributed uniformly over a thick shell. For intermediate temperatures, all C-atoms are distributed over the surface of C_{70} molecule and for low temperatures, where all the rotations freeze out, the total interaction can be found by pair wise sum of all the 70 C-atom-atom potentials on all the molecules. The work in this direction is in progress and will be reported.

Acknowledgements:

The authors gratefully acknowledge the financial support for the research project “Phonon Dynamics of Fullerenes and Derivatives”, SP/S2/M13/96 from the Department of Science and Technology, Government of India, New Delhi, India under which the present work was done.

REFERENCES

1. Science of Fullerenes and Carbon Nanotubes (by Dresselhaus M.S., Dresselhaus G. and Eklund P.C.) Acad. Press, NY (1996).
2. G.B.Vaughan, P.A.Heiney, J.E.Fisher, D.E.Luzzi, D.A.Rickets-Foot, A.R.McGhie, Y.W.Hui, A.L.Smith, D.E.Cox, W.J.Romanow, B.H.Allen, N.Coustel, J.P.McCauley, Jr., and A.B.Smith III.*Science*, **254**, 1350 (1991).
3. M.A.Verheijen, H.Meeke, G.Meijer, P.Bennema, J.L.deBoer, S.van Smmalen, G.V.Tendeloo, S.Amelinckx, S.Muto, and J.van Landuyt. *Chem. Phys.*, **166**, 287 (1992).
4. H.Kawamura, Y.Akahama, M.Kobayashi, H.Shinohara, H.Sato, Y.Saito, T.Kikegawa, O.Shimomura, and K.Aoki.*J. Phys. Chem. Solids*, **54**, 1675(1993).
5. M. Pickholz and Z. Gamba, *Phys. Rev. B*, **53**, 2159 (1996).
6. R. Sachidanandam, T.C. Lubensky, and A.B. Harris, *Phys. Rev. B*, **51**, 12380 (1995).
7. Jindal V.K., Dharamvir K. and Sarbpreet Singh, *Int. J. Mod. Phys.* **B14**, 51-69 (2000).
8. A.V.Nilolaev, T.J.S.Dennis, K.Prassides and A.K.Soper, *Chem Phys. Lett.*, **223**,143 (1994).
9. C.Z.Wang,C.T.Chan and K.M.Ho. *Phys. Rev. B*, **46**, 9761 (1992).
10. W.Andreoni, F.Gygi and M.Parrinello, *Chem. Phys. Lett.*, **189**, 241 (1992).
11. K.Ranghavachari and C.M.Rohlfing. *J.Phys.Chem.*, **95**, 5768(1991).
12. C.Pan *et al.*, *J.Phys. Chem.* **95**, 2944 (1991).

APPENDIX

As discussed earlier at higher temperature rugby ball shaped C_{70} molecule can be replaced by a thick spherical shell and the interaction potential can be obtained by integrating over the two shells instead of atom-atom summation. As already discussed for this case we can write the interaction potential by considering the two volume elements dV_1 and dV_2 with position vectors \mathbf{r}_1 and \mathbf{r}_2 on two shells as given by equation (5), where ρ is the density of carbon atoms within the thick shell volume and dV_1 and dV_2 are taken as the volumes of the thick ring along the shell surfaces and are given by

$$dV_1 = (2\pi r_1 \sin \theta_1) \cdot r_1 d\theta_1 \cdot dr_1 \quad \text{A1}$$

$$\text{and } dV_2 = 2\pi(r_2 - r) \sin \theta_2 \cdot (r_2 - r) d\theta_2 \cdot dr_2 \quad \text{A2}$$

where R is the distance between the centers of the two shells. Substituting these values in equation (5) and integrating over the two volumes the final equation for the total interaction between the two shells can be obtained very easily and is represented by

$$V(r,a,b) = U_{\text{att}} + U_{\text{rep}} \quad \text{A3}$$

where U_{att} and U_{rep} are the attractive and the repulsive contributions and are given by

$$U_{\text{att}} = \pi^2 \rho^2 A U'_{\text{att}}$$

where $U'_{\text{att}} =$

$$\begin{aligned} & \frac{b}{2R} \log \left| \frac{(R-2b)(R+a+b)(R+a-b)}{(R+2b)(R-a+b)(R-a-b)} \right| + \frac{1}{2} \log \left| \frac{R^2(R+a+b)(R-a-b)}{(R+2b)(R-2b)(R-a+b)(R+a-b)} \right| \\ & + \frac{a}{2R} \log \left| \frac{(R-2a)(R+a+b)(R-a+b)}{(R+2a)(R-a-b)(R+a-b)} \right| + \frac{1}{2} \log \left| \frac{R^2(R+a+b)(R-a-b)}{(R+2a)(R-2a)(R+a-b)(R-a+b)} \right| \\ & + \frac{1}{6R} \left[(3b+2R) \log \left| \frac{(R+2b)(R-a+b)}{R(R+a+b)} \right| + (b^2+bR) \left(\frac{1}{R+2b} - \frac{1}{R} - \frac{1}{R+a+b} + \frac{1}{R-a+b} \right) \right] \\ & - \frac{1}{6R} \left[(3a+2R) \log \left| \frac{R(R+a+b)}{(R+2a)(R+a-b)} \right| + (a^2+aR) \left(\frac{1}{R+a+b} - \frac{1}{R+2a} - \frac{1}{R+a-b} + \frac{1}{R} \right) \right] \\ & + \frac{1}{6R} \left[(3b-2R) \log \left| \frac{R(R-a-b)}{(R+a-b)(R-2b)} \right| + (-b^2+bR) \left(\frac{1}{R} - \frac{1}{R+a-b} - \frac{1}{R-2b} + \frac{1}{R-a-b} \right) \right] \\ & - \frac{1}{6R} \left[(3a-2R) \log \left| \frac{(R+b-a)(R-2a)}{R(R-a-b)} \right| + (-a^2+aR) \left(\frac{1}{R-a+b} - \frac{1}{R} - \frac{1}{R-a-b} + \frac{1}{R-2a} \right) \right] \end{aligned}$$

A4

$$U_{\text{rep}} = -\frac{4\pi^2 \rho^2 B}{\alpha^2} \cdot U'_{\text{rep}}$$

where $U'_{\text{rep}} =$

$$\begin{aligned} & \left[\begin{aligned} & -(b^2\alpha^2 + 2b\alpha + 2)e^{-\alpha(R+2b)} + (a^2\alpha^2 + 2a\alpha + 2)e^{-\alpha(R+a+b)} - (\alpha R + 2)(b\alpha + 1)e^{-\alpha(R+2b)} \\ & + (\alpha R + 2)(a\alpha + 1)e^{-\alpha(R+a+b)} + (b^2\alpha^2 - 2b\alpha + 2)e^{-\alpha R} - (a^2\alpha^2 - 2a\alpha + 2)e^{-\alpha(R-a+b)} \\ & - (\alpha R + 2)(b\alpha - 1)e^{-\alpha R} + (\alpha R + 2)(a\alpha - 1)e^{-\alpha(R-a+b)} \end{aligned} \right] \\ & - \left[\begin{aligned} & -(b^2\alpha^2 + 2b\alpha + 2)e^{-\alpha(R+a+b)} + (a^2\alpha^2 + 2a\alpha + 2)e^{-\alpha(R+2a)} - (\alpha R + 2)(b\alpha + 1)e^{-\alpha(R+a+b)} \\ & + (\alpha R + 2)(a\alpha + 1)e^{-\alpha(R+2a)} + (b^2\alpha^2 - 2b\alpha + 2)e^{-\alpha(R+a-b)} - (a^2\alpha^2 - 2a\alpha + 2)e^{-\alpha R} \\ & - (\alpha R + 2)(b\alpha - 1)e^{-\alpha(R+a-b)} + (\alpha R + 2)(a\alpha - 1)e^{-\alpha R} \end{aligned} \right] \\ & + \left[\begin{aligned} & -(b^2\alpha^2 + 2b\alpha + 2)e^{-\alpha R} + (a^2\alpha^2 + 2a\alpha + 2)e^{-\alpha(R+a-b)} - (\alpha R + 2)(b\alpha + 1)e^{-\alpha R} \\ & + (\alpha R + 2)(a\alpha + 1)e^{-\alpha(R+a-b)} + (b^2\alpha^2 - 2b\alpha + 2)e^{-\alpha(R-2b)} - (a^2\alpha^2 - 2a\alpha + 2)e^{-\alpha(R-a-b)} \\ & - (\alpha R + 2)(b\alpha - 1)e^{-\alpha(R-2b)} + (\alpha R + 2)(a\alpha - 1)e^{-\alpha(R-a-b)} \end{aligned} \right] \\ & - \left[\begin{aligned} & -(b^2\alpha^2 + 2b\alpha + 2)e^{-\alpha(R-a+b)} + (a^2\alpha^2 + 2a\alpha + 2)e^{-\alpha R} - (\alpha R + 2)(b\alpha + 1)e^{-\alpha(R-a+b)} \\ & + (\alpha R + 2)(a\alpha + 1)e^{-\alpha R} + (b^2\alpha^2 - 2b\alpha + 2)e^{-\alpha(R-a-b)} - (a^2\alpha^2 - 2a\alpha + 2)e^{-\alpha(R-2a)} \\ & - (\alpha R + 2)(b\alpha - 1)e^{-\alpha(R-a-b)} + (\alpha R + 2)(a\alpha - 1)e^{-\alpha(R-2a)} \end{aligned} \right] \\ & + \left[\begin{aligned} & \frac{b^2\alpha^2 + 2b\alpha + 2}{\alpha^5 R} \left[-(b\alpha + 1)e^{-\alpha(R+2b)} + (a\alpha + 1)e^{-\alpha(R+a+b)} - (b\alpha - 1)e^{-\alpha R} + (a\alpha - 1)e^{-\alpha(R-a+b)} \right] \\ & - \frac{a^2\alpha^2 + 2a\alpha + 2}{\alpha^5 R} \left[-(b\alpha + 1)e^{-\alpha(R+a+b)} + (a\alpha + 1)e^{-\alpha(R+2a)} - (b\alpha - 1)e^{-\alpha(R+a-b)} + (a\alpha - 1)e^{-\alpha R} \right] \\ & - \frac{b^2\alpha^2 - 2b\alpha + 2}{\alpha^5 R} \left[-(b\alpha + 1)e^{-\alpha R} + (a\alpha + 1)e^{-\alpha(R+a+b)} - (b\alpha - 1)e^{-\alpha(R-2b)} + (a\alpha - 1)e^{-\alpha(R-a-b)} \right] \\ & + \frac{a^2\alpha^2 - 2a\alpha + 2}{\alpha^5 R} \left[-(b\alpha + 1)e^{-\alpha(R-a+b)} + (a\alpha + 1)e^{-\alpha R} - (b\alpha - 1)e^{-\alpha(R-a-b)} + (a\alpha - 1)e^{-\alpha(R-2a)} \right] \end{aligned} \right] \end{aligned}$$

A5

These expressions have been used for the calculations of potential energies.